

ADSORPTION-COUPLED REDUCTION OF HEXAVALENT CHROMIUM BY JUTE-BASED ANIONIC ADSORBENT FROM AQUEOUS SOLUTIONS

CANHUI DENG, ZEMAO YANG, ZHIGANG DAI, CHAOHUA CHENG, QING TANG, YING XU, CHAN LIU, JIQUAN CHEN, DONGWEI XIE and JIANGUANG SU

Institute of Bast Fiber Crops, Chinese Academy of Agricultural Science, 348 West XianJiahu Road, Changsha, 410082, PR China

✉ *Corresponding author: S. Jianguang, jgsu@vip.163.com, dengcanhui@caas.cn*

Received August 7, 2019

A new efficient anion adsorbent was fabricated by amino-grafting lignocellulose-rich jute stalk (AGJ) to uptake toxic hexavalent chromium (Cr(VI)) from aqueous solutions. Batch adsorption experiments were performed as a function of adsorbent dosage and initial solution pH to test the adsorption-coupled reduction for anion Cr(VI). Maximum chromium adsorption was found at pH 2.0 with an appropriate adsorbent dosage of 1.0 g/L. The adsorption equilibrium data were best described by the Langmuir isotherm model. The maximum monolayer adsorption capacity was 154.30 mg/g, evaluated using the Langmuir equation. The kinetic analysis revealed that the adsorption of Cr(VI) was fitted very well by the pseudo-second-order model during the whole adsorption process. The binding mechanism of chromium onto the AGJ surface was confirmed by Fourier transform infrared spectroscopy (FTIR) and X-ray photoelectron spectroscopy (XPS) analyses. All the results in this study illustrated that AGJ could be considered as an economically viable and effective adsorbent for treatment of aqueous solutions contaminated with Cr(VI).

Keywords: jute stalk, adsorption-coupled reduction, Cr(VI), kinetics, equilibrium

INTRODUCTION

Chromium, which is considered one of the top-priority toxic pollutants because of its teratogenic and carcinogenic effects in humans, exists in the environment mainly in two oxidation states, trivalent chromium (Cr(III)) and hexavalent chromium (Cr(VI)).¹ Compared to Cr(III), Cr(VI) is more hazardous and toxic, owing to the highly soluble and mobile forms of hydrogen chromate (HCrO_4^-), dichromate ($\text{Cr}_2\text{O}_7^{2-}$) and chromate (CrO_4^{2-}) ions in water streams.² Cr(VI) is widely generated from various industrial processes, such as electroplating, pharmacy, metallurgy, textiles, battery and catalyst synthesis.³ The world health organization (WHO) recommends that the tolerance limit for Cr(VI) should be 0.05 mg/L for discharge into potable water, 0.1 mg/L into inland surface water, and 0.25 mg/L into industrial wastewater.⁴ Therefore, it is of critical importance to remove or reduce the concentration of Cr(VI) before its discharge into aquatic environments.

Several treatment techniques have been

developed for removal of Cr(VI) from aqueous solutions, including reduction-precipitation,⁵ membrane separation (ultrafiltration, reverse osmosis and nanofiltration),^{6,7} electrolytic recovery,⁸ ion exchange/chelation,⁹ microbial remediation and adsorption.^{10,11} Of these methods, adsorption has been increasingly considered as an effective and versatile alternative for eliminating Cr(VI) from water and wastewaters. Activated carbon has been employed as a common adsorbent for the treatment of contaminants in aqueous solutions, but it is prohibitively expensive.¹² Therefore, low-cost adsorbents should be exploited for a simple and efficient adsorption in water and wastewater treatment. Recently, agricultural and industrial by-products, such as corn stalk,¹³ wheat straw,¹⁴ rice bran,¹⁵ sugar waste,¹⁶ coffee residues,¹⁷ and hydrolyzed lignocellulosic materials obtained from bioethanol production,¹⁸ have attracted the attention of scientists due to their naturally occurring, low-cost, abundant production and

lignocellulose-rich content, as well as efficient adsorption to some extent. In addition, Sarkar *et al.* reported that water hyacinth shoot powder could be a potential adsorbent for removal of Cr and Cu, with high adsorbent capacity of about 99% Cr and Cu from a standard solution (SS), as well as from tannery effluent (TE).¹⁹

Jute is also an abundant agricultural waste, rich in cellulose and lignocelluloses, which has three hydroxyl groups at the anhydroglucose units of the cellulose backbone. Thus, it provides the possibility for application as adsorbent.²⁰ However, the jute adsorbent lacks high adsorption capacity toward heavy metal contaminants in its native form. It was reported that the metal ion uptake reached values of only 4.23, 3.37 and 3.55 mg g⁻¹ for Cu(II), Ni(II) and Zn(II), respectively, by jute fibres.²¹ With the aim of enhancing the adsorption capacity, chemically modified cellulose adsorbent has been synthesized. Hao *et al.* prepared a novel amino-functionalized cellulose adsorbent in an ionic liquid homogeneous system, which displayed a high removal efficiency for Cr(VI), with optimal Cr(VI) uptake of 32.5 mg g⁻¹.²² Du *et al.* have reported the preparation of a low-cost carboxyl modified jute fiber for removal of Pb(II), Cd(II), and Cu(II) from water, with remarkably high adsorption capacity (157.21, 88.98 and 43.98 mg g⁻¹ for Pb(II), Cd(II), and Cu(II), respectively).²³

The main objective of this work has been to investigate the potential use of an anionic adsorbent synthesized from jute stalks through amino-functionalization of natural cellulose in removing Cr(VI) anion species from water. The prepared anionic adsorbent from jute stalks was characterized by chemical analysis and the effects of important parameters, including adsorbent dosage and initial pH of the solution, were conducted using batch experiments. The potential application of functionalized jute stalks for adsorption of Cr(VI) from water was investigated under kinetic and equilibrium conditions. The mechanism of Cr(VI) adsorption onto the jute-based adsorbent was determined by several kinetic and isotherm adsorption models. The interaction between Cr(VI) and the adsorbent was eliminated by FTIR and XPS analyses.

EXPERIMENTAL

Preparation of amine grafted jute

The raw jute was obtained from the experimental

field of the Institute of Bast Fiber Crops, Chinese Academy of Agricultural Sciences, China. It was washed with de-ionized (DI) water, dried in sunlight until all the moisture was evaporated. Then, the raw jute was smashed to pieces and sieved to the desired mesh size of 100~300 µm. For preparation of amine grafted jute (AGJ), a 250 mL three-neck round bottom flask was employed, and then two grams of raw jute powder, 10 mL of epichlorohydrin and 12 mL of N,N-dimethylformamide were mixed in it and stirred for 1 h at 100 °C. After addition of 2 mL of diethylenetriamine drop by drop, the mixture was stirred for another 1 h, followed by the addition of 10 mL of triethylamine and stirring for 3 h. The primary product was washed with DI water, freeze-dried for 24 h, and then sieved to an appropriate mesh size of 100~300 µm. Finally, the obtained samples were stored in desiccators as adsorbents.

Characterization of adsorbents

The morphologies of raw jute and AGJ were observed by scanning electron microscopy (SEM) using a JSM-5600 LV microscope (JEO, Ltd., Japan). The BET surface area was determined by an ASAP 2020 Accelerated Surface Area and Porosimetry System (Micromeritics Instrument Corporation, USA). Infrared adsorption spectra were recorded on a Fourier transform infrared (FTIR) spectrometer (IRAffinity-1, Shimadzu) at room temperature, in the range from 400 to 4000 cm⁻¹. The composition and binding energy information of AGJ and AGJ loaded with Cr(VI) were investigated by X-ray photoelectron spectroscopy (XPS), using a Thermo Scientific Escalab 250Xi spectrometer equipped with a monochromic Mg K α X-ray source. Detailed spectra processing was performed by commercial Thermo Avantage software (v. 5.52, Thermo Scientific).

Adsorption experiments

All adsorption experiments were conducted in sealed 50 mL conical flasks that contained 20 mg AGJ and 20 mL Cr(VI) solution with appropriate concentrations. The flasks were placed on an incubator at 150 rpm shaking speed at an appropriate temperature. After adsorption, samples were drawn out from the flasks and then filtered through a 0.45 µm membrane filter. The residual concentration of Cr(VI) in the filtrate was analyzed using a UV-vis spectrophotometer (Shimadzu UV-2550, Japan). The pink complex formed from Cr(VI) and 1,5-diphenylcarazide was determined at the maximum adsorption wavelength of 540 nm.²⁴ The amount adsorbed (q_e , mg/g) was calculated as follows:

$$q_e = \frac{(C_0 - C_e)V}{m} \quad (1)$$

where C_0 and C_e are the initial and equilibrium

concentrations of Cr(VI) (mg/L), V is the solution volume (L), and m is the mass of adsorbent (g).

In the dosage experiments, 5~80 mg dosages of AGJ were added into batches of 20 mL of Cr(VI) solution with the concentration of 100 mg/L under stirring conditions for 4 h at natural pH. The effect of pH on the adsorption of AGJ was investigated by mixing 20 mg of AGJ with 20 mL of 100 mg/L Cr(VI) solution at different initial pH values of 2~9. The solution pH was adjusted with 0.5 M NaOH or HCl solution. To determine the minimum time required for reaching adsorption equilibrium, adsorption kinetics studies were carried out with various concentrations of Cr(VI) (50, 100 and 200 mg/L) at 25 °C. The concentrations of Cr(VI) were analyzed at given time intervals from 1 min to 4 h. The adsorption isotherms of Cr(VI) on AGJ were obtained at 25 °C, 35 °C and 45 °C, respectively, to evaluate the thermodynamic properties and the maximum adsorption. Typically, 20 mL of Cr(VI) with initial concentrations ranging from 10 to 500 mg/L were mixed with 20 mg of AGJ, and

shaken for 4 h at constant temperature to attain equilibrium. After filtering separation, the Cr(VI) concentrations were measured.

RESULTS AND DISCUSSION

Characterization

The morphologies of raw jute and AGJ were observed using SEM. As shown in Figure 1, the surface of AGJ was relatively smoother than that of raw jute, suggesting the order of cellulose in jute has been improved during the amination reaction. The BET measurement revealed that the specific surface areas of raw jute and AGJ were $75.84 \text{ m}^2 \text{ g}^{-1}$ and $52.03 \text{ m}^2 \text{ g}^{-1}$, respectively. The BET surface area of AGJ decreased after grafting with amine groups, which is consistent with the results of SEM analysis. These results are similar to those from a previous report.²⁵

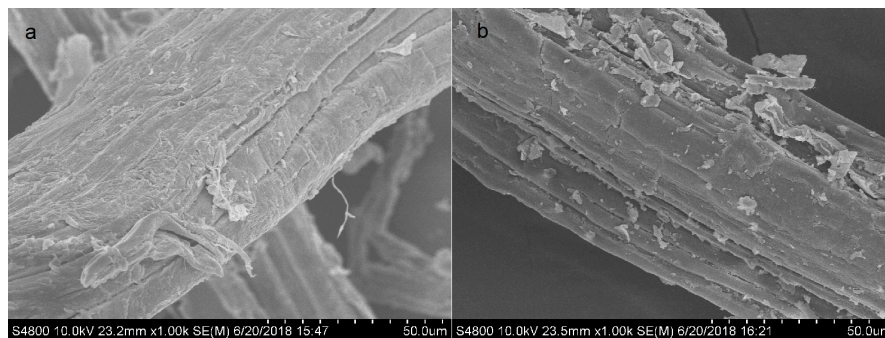


Figure 1: SEM images of raw jute (a) and AGJ (b)

FTIR spectral analysis is important to identify the characteristic functional groups, which are responsible for the adsorption of metal ions.²⁶ The FTIR spectra of AGJ and Cr(VI) laden AGJ are displayed in Figure 2. It is apparent that there were some changes in the peak frequencies observed from the FTIR spectra. The spectrum of AGJ exhibits an absorption band at 3433 cm^{-1} , which corresponds to the bonded -OH stretching vibration. After adsorption of Cr(VI), it shifted to 3419 cm^{-1} in the spectrum of Cr(VI) laden AGJ, partially owing to complexation of Cr(VI) with -OH groups.²⁷ The appearance of a new peak at 892 cm^{-1} in the spectrum of Cr(VI) laden AGJ indicates the adsorption of Cr(VI) on AGJ. A similar phenomenon has been reported by Ren *et al.*²⁸ In the AGJ spectrum, the band at 1058 cm^{-1} corresponds to the C-O-C stretching vibration of

the cellulose backbone.²⁹ The broad band observed at 1641 and 1370 cm^{-1} could be assigned to the carboxyl and amine groups.³⁰ After Cr(VI) binding, the characteristic peaks at 1641 and 1370 cm^{-1} shifted to 1646 and 1372 cm^{-1} , respectively, indicating that amino and carboxyl groups contributed to the adsorption of Cr(VI). These results suggest that the adsorption of Cr(VI) onto AGJ could be ascribed to the complex interactions between Cr(VI) and AGJ, including electrostatic attraction, complexation, as well as ion exchange.

Cr(VI) adsorption tests

Effect of adsorbent dose on Cr(VI) adsorption

The effect of AGJ dosage on Cr(VI) adsorption is shown in Figure 3. It can be noted that the uptake of Cr(VI) increased rapidly with the increasing dosage of AGJ adsorbent from 0.25 to

1.5 g/L. In this period, more Cr(VI) ions were removed, which could be ascribed to higher surface area and more active sites for Cr(VI) adsorption provided by increasing the AGJ dosage. The removal efficiency of Cr(VI) was maintained high (95~100%) as the dosage of AGJ was

increased from 1.5 to 4.0 g/L. However, the adsorption capacity (q_e) of Cr(VI) by the AGJ adsorbent decreased from 116.3 to 27.7 mg/g, while increasing the AGJ dosage from 0.25 to 4.0 g/L. Therefore, an optimum dosage of 1.0 g/L was selected for subsequent adsorption experiments.

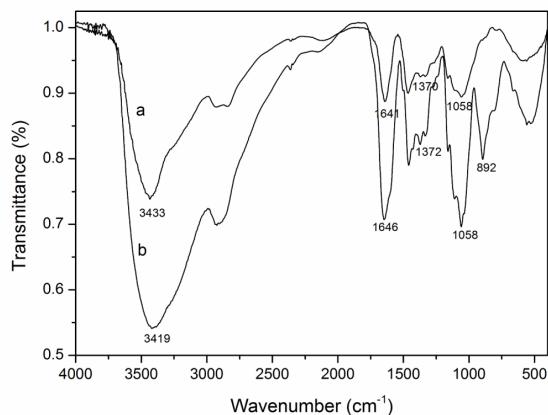


Figure 2: FTIR spectra of (a) AGJ and (b) Cr laden AGJ

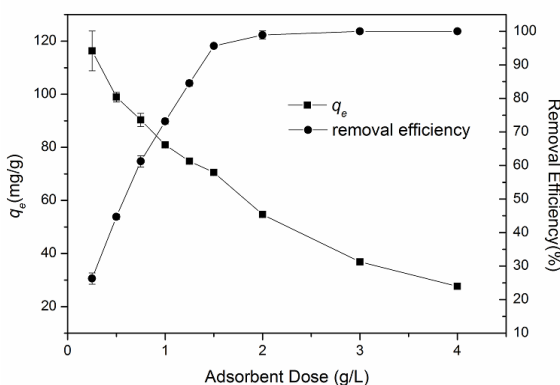


Figure 3: Effect of AGJ dosage on Cr(VI) adsorption (20 mL of 100 mg/L Cr(VI) solution used with 0.25 to 4.0 g/L of AGJ for 4 h)

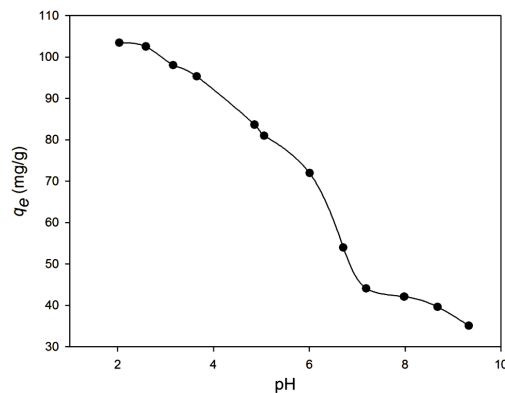


Figure 4: Adsorption performance of AGJ at different initial pH of Cr(VI) solution (20 mg AGJ used with 20 mL of 100 mg/L Cr(VI) solution at different initial pH values of 2~9 for 4 h)

Effect of pH on Cr(VI) adsorption

The pH is one of the most important factors for metal adsorption onto adsorbents from aqueous solution. The adsorption of Cr(VI) onto AGJ as a function of pH is illustrated in Figure 4. It can be noted that the uptake of Cr(VI) decreased from 103.42 mg/g to 35.07 mg/g with increasing pH from 2.04 to 9.33. There are various forms of Cr(VI) in aqueous solution, such as HCrO_4^- , $\text{Cr}_2\text{O}_7^{2-}$, CrO_4^{2-} , *etc.* The chromate anions HCrO_4^- and $\text{Cr}_2\text{O}_7^{2-}$ are predominant between pH 2.0 and 6.0, while CrO_4^{2-} is predominant above pH 6.0.²⁵ It suggests that one adsorption site from AGJ was required for the

adsorption of dominant HCrO_4^- at lower pH, while two adsorption sites were necessary for the adsorption of divalent $\text{Cr}_2\text{O}_7^{2-}$ or CrO_4^{2-} at high pH.³¹ Therefore, there was a higher adsorption capacity of Cr(VI) ions by AGJ at lower pH than at relatively higher pH.

In addition, at lower pH, the protonation of the amino groups grafted onto AGJ was enhanced, and as a result, more negatively charged Cr(VI) ions were attracted by more positively charged hydronium ions (H^+) on the surface of AGJ. In contrast, at higher pH, the OH^- anion was increased with the increasing pH, which resulted in repulsion between the OH^- and the negatively

charged Cr(VI) ions, which led to a decreasing adsorption capacity for Cr(VI).³²

Adsorption kinetics

The adsorption kinetics of Cr(VI) by AGJ at different Cr(VI) concentration is shown in Figure 5. It is worth noting that the adsorption rate increased dramatically within the first 10 min and the adsorbed amount of Cr(VI) reached 48.56, 79.14 and 98.92 mg/g, when the initial Cr(VI) concentration was 50, 100 and 200 mg/g, respectively. The rapid uptake in the initial stage could be attributed to the high concentration gradient, which displayed a high driving force for migration of Cr(VI) from the solution onto the surface of AGJ. Subsequently, the adsorption rate was observed to be slow and an apparent equilibrium was achieved. The equilibrium time for adsorption of Cr(VI) onto the surface of AGJ was found to be around 60 min for different concentrations of Cr(VI).

In order to understand the mechanism involved in the adsorption process, the adsorption kinetics was examined. Numerous kinetic models provide an insight into the reaction order of adsorption based on the capacity of the adsorbent and the

solution concentration.³³ To evaluate the adsorption kinetics of Cr(VI) onto AGJ, several models have been employed: the Lagergren pseudo-first-order model and pseudo-second-order model and the Elovich equation model.

The pseudo-first-order model and the pseudo-second-order model are described by Equation 2 and Equation 3, while the Elovich equation is presented in Equation 4:

$$q_t = q_e (1 - e^{-k_1 t}) \quad (2)$$

$$q_t = \frac{t}{\frac{1}{k_2 q_e^2} + \frac{t}{q_e}} \quad (3)$$

$$q_t = \frac{1}{\beta} \ln(\alpha\beta) + \frac{1}{\beta} \ln(t) \quad (4)$$

where q_e and q_t (mg/g) are adsorption capacity at equilibrium and time t (min), respectively; k_1 (min^{-1}), and k_2 ($\text{g mg}^{-1} \text{min}^{-1}$) are the rate constant of pseudo-first-order, pseudo-second-order model and intra-particle diffusion model, respectively; Elovich kinetic constants, α ($\text{mg}(\text{g min})^{-1}$) is the initial adsorption rate, and β (g mg^{-1}) is the desorption constant.

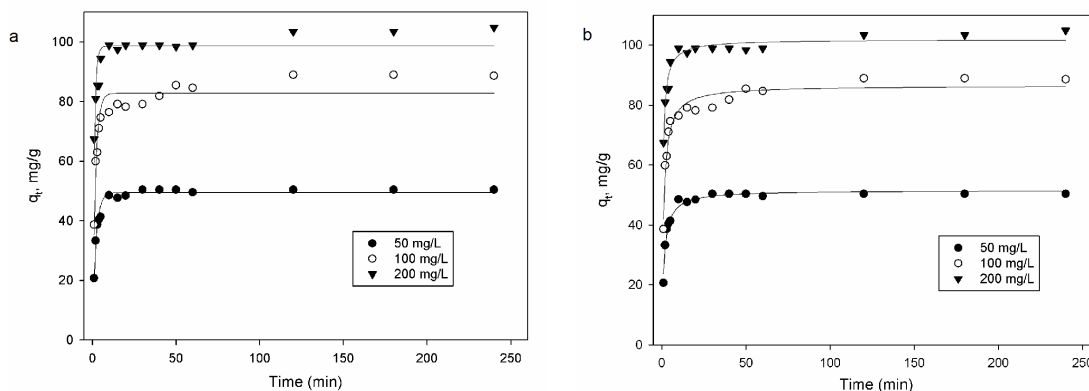


Figure 5: Adsorption kinetic data of Cr(VI) at different concentration of 50, 100 and 200 mg/L onto AGJ, fitted by pseudo-first-order (a) and pseudo-second-order model (b)

All the corresponding kinetic parameters from the four models for different concentrations are presented in Table 1. It was observed that the pseudo-first-order model showed relatively small values of correlation coefficients (R^2), indicating the limitations of the boundary layer in controlling the adsorption process. It is known that the pseudo-first-order kinetic model is

generally applicable to the adsorption process at the initial stage, but does not fit well to the whole process in many cases.³⁴ However, the R^2 values were close to 1 for all Cr(VI) concentrations, when the experimental data fitted the pseudo-second-order model, which suggested that the rate-controlling process of the adsorption could be chemical adsorption, involving valence

forces by exchange or sharing electrons between the adsorbate and the adsorbent.

The Elovich equation was applied to describe the chemical reaction mechanism involving the rate-controlling process of adsorption.³⁵ As can be seen from Table 1, the initial adsorption rate constant α increased with initial Cr(VI) concentration, owing to the higher driving force. The desorption constant β should decrease with initial concentration because of less available surface for Cr(VI), which was not consistent with the result obtained in this research, indicating that the Elovich equation was not suitable for describing the adsorption kinetics of Cr(VI) onto AGJ.

Adsorption isotherms

The adsorption equilibrium of Cr(VI) onto AGJ was evaluated at different temperatures to assess the adsorption capacity of the latter. Three important isotherm models were employed in this research to analyze the batch experimental data: the Langmuir, Freundlich and Temkin isotherm models.

The Langmuir model is based on the monolayer kinetic equilibrium between adsorption and desorption, as follows:³⁶

$$q_e = \frac{q_m K_L C_e}{1 + K_L C_e} \quad (5)$$

The Freundlich model is an empirical multilayer adsorption isotherm for non-ideal adsorption onto heterogeneous surfaces, and it has the following form:³⁷

$$q_e = K_F C_e^{1/n} \quad (6)$$

The Temkin equation is:

$$q_e = B \ln A + B \ln C_e \quad (7)$$

where q_e (mg/g) and C_e (mg/L) are related to the equilibrium concentrations in the solid phase and fluid phase, respectively. In the Langmuir model, q_m (mg/g) is the maximum adsorption capacity of the monolayer, K_L (L/mg) is the equilibrium constant. In the Freundlich model, K_F (mg/g(L/mg)^{1/n}) and $1/n$ are related to the adsorption capacity and adsorption intensity, respectively. The parameter $1/n$ must be between 0 and 1. In the Temkin model, A (mg/L) is the equilibrium binding constant and B is the Temkin constant related to the heat of adsorption.

All the constants and correlation coefficients obtained from the three isotherm models for Cr(VI) adsorption onto AGJ are summarized in

Table 2. The adsorption isotherm data of Cr(VI) at different temperatures fitted with the Langmuir model are shown in Figure 6. On the basis of the correlation coefficients (R^2), the Langmuir model gave the highest R^2 values, which were greater than 0.96 at all the three temperatures tested, showing that the Langmuir model yields the best fit, among the isotherms examined here. This result indicates that a monomolecular layer was formed without any interactions between the adsorbed molecules in the adsorption process of Cr(VI). The value of q_m , calculated from the Langmuir equation, increased with the increasing temperature, and reached 154.30 mg/g at 40 °C, which confirmed that the adsorption process for Cr(VI) onto AGJ was an endothermic reaction.

For the Freundlich model, the value of $1/n$ ranged between 0 and 1 at all temperatures, indicating favorable adsorption of Cr(VI) onto AGJ. Similar results have been reported in the adsorption of Cr(VI) onto a new ion-exchanger derived from wheat straw.³³ The Temkin constant B increased with the increase in the solution temperature, also suggesting the endothermic property of the Cr(VI) adsorption process.³⁸

Uptake mechanism

XPS is one of the most useful tools for analyzing the adsorption interaction and the defining adsorption mechanisms.³⁹ XPS spectra could be employed to determine particular elements and to identify the valence state of metals laden on AGJ. XPS analysis of AGJ before and after adsorption of Cr(VI) is depicted in Figure 7. As indicated in Figure 7a, the elemental composition of AGJ was determined and the peaks were successfully assigned to the corresponding carbon, oxygen, nitrogen and chromium atoms. Compared to AGJ, new peaks of Cr 2p appeared in the Cr laden AGJ, indicating the successful adsorption of Cr(VI) onto the surface of the AGJ composite.

As shown in Figure 7a, after AGJ adsorbed Cr(VI), two new peaks appeared at binding energies of 585.9 eV and 576.2 eV. As may be noticed in the magnified Figure 7b, the peaks at 585.9 eV and 576.2 eV were characteristic peaks of Cr 2p_{1/2} and Cr 2p_{3/2}, which suggests the presence of Cr(III) in AGJ after adsorption.⁴⁰

Table 1
Kinetic data and correlation coefficient R^2 obtained from kinetic models

C_0 (mg L^{-1})	Pseudo-first order		Pseudo-second order		Elovich			Intra-particle diffusion	
	K_1 (min^{-1})	R^2	K_2 ($\text{g}(\text{mg min})^{-1}$)	R^2	α ($\text{mg}(\text{g min})^{-1}$)	β (g mg^{-1})	R^2	k_p ($\text{mg}(\text{g min})^{-1}$)	R^2
50	0.1656	0.8879	0.0236	0.9999	8.63×10^1	0.0856	0.9532	11.6965	0.8521
100	0.2126	0.8267	0.0110	0.9992	1.74×10^2	0.0535	0.9299	18.9846	0.8097
200	0.4180	0.8702	0.0073	0.9991	2.25×10^3	0.0736	0.9498	13.7857	0.8733

Table 2
Isotherm parameters obtained for Cr(VI) adsorption by AGJ

Isotherm models	Parameters	Temperature		
		25 °C	35 °C	45 °C
Langmuir	q_m (mg/g)	137.53	151.79	154.30
	K_L (L/mg)	0.0116	0.0098	0.0096
	R^2	0.9823	0.9657	0.9767
Freundlich	K_F ($\text{mg/g}(\text{L/mg})^{1/n}$)	10.6883	9.3307	9.5478
	$1/n$	0.4013	0.4314	0.4315
	R^2	0.9011	0.9134	0.9206
Temkin	A (mg/L)	0.1092	0.1024	0.1009
	B	30.5584	32.3793	33.1076
	R^2	0.9806	0.9593	0.9689

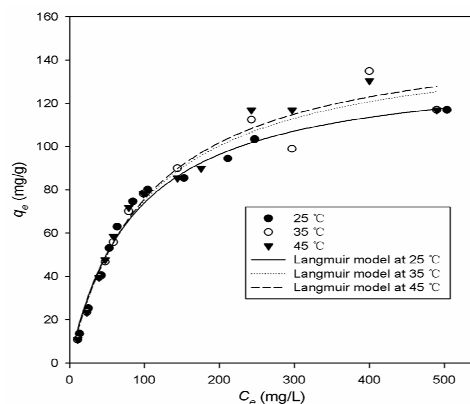


Figure 6: Adsorption isotherm of Cr(VI) at different temperature of 25, 35 and 40 °C onto AGJ, fitted by Langmuir model

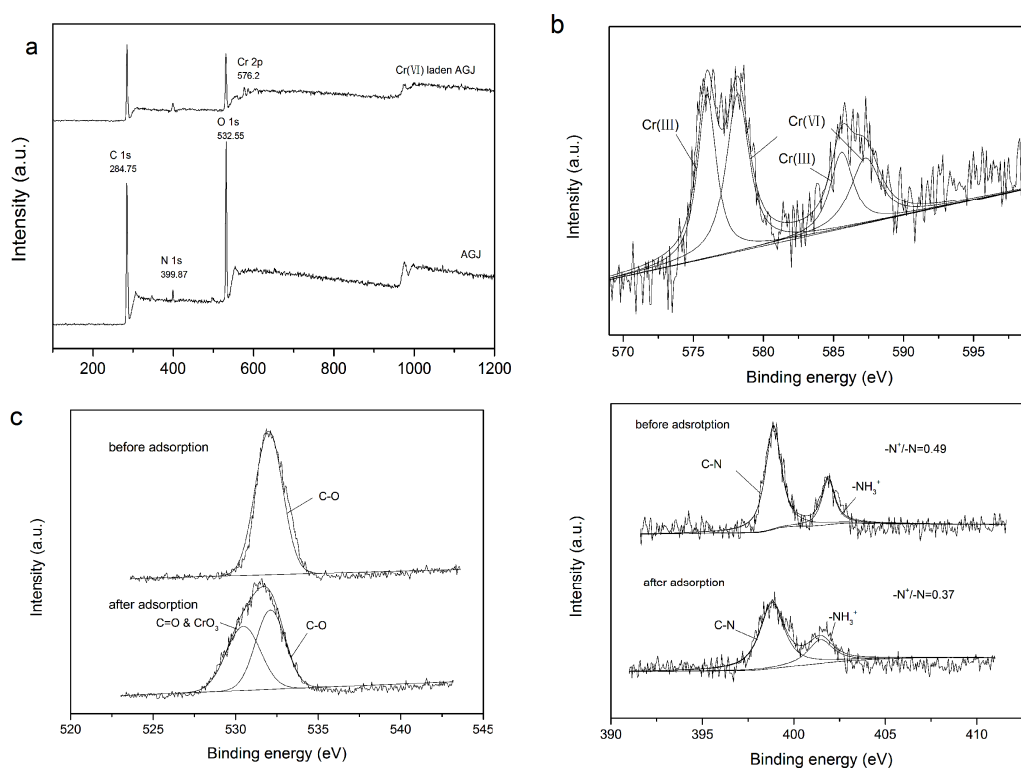


Figure 7: Wide scan XPS spectra of AGJ and Cr laden AGJ (a); Cr 2p on the AGJ surface after adsorption (b); O 1s (c) and N 1s (d) on the AGJ surface before and after adsorption

The peak of Cr $2p_{3/2}$ at the binding energy of 576.2 eV could be fitted into two peaks at 576.0 and 578.1 eV, which was attributed to Cr(III)-OH and Cr(VI)-O. The peak of Cr $2p_{1/2}$ at the binding energy of 585.9 eV could be also fitted into two peaks at 585.6 and 587.3 eV, which was assigned to Cr(III)-OH and Cr(VI)-O in $\text{Cr}_2\text{O}_7^{2-}$ or HCrO_4^- , respectively. These results indicated that a part of the laden Cr(VI) on the AGJ surface was reduced to the less toxic Cr(III), and AGJ also has an

adsorption capacity for Cr(III).⁴¹

To further study the uptake mechanism of Cr(VI) by AGJ, the chemical status of O 1s and N 1s species on the adsorbent surface before and after Cr(VI) adsorption was also explored. As shown in Figure 7c, the band at 532.3 eV corresponding to the peak of C-O was lowered to a certain extent and some new peaks of C=O, CrO_3 and Cr(OH)_3 appeared after the adsorption of Cr(VI). These results suggested that chromium

might bind to ligands containing oxygen, such as hydroxyl, carboxyl or phenolic groups, present on the surface of AGJ. In addition, the peak of C=O increased obviously, which was due to the oxidation of the -OH group, implying that the hydroxyl groups were the electron donor during the process of Cr(VI) reduction to Cr(III). Also, the high resolution spectra of N 1s from AGJ before and after Cr(VI) adsorption are showed in Figure 7d. It can be noted that there are two obvious peaks in the spectrum of N 1s from AGJ (see Fig. 3b) at binding energies of 398.8 and 401.7 eV, which were attributed to N atoms bonded with C atoms (C-N) and to -NH_3^+ , respectively.²⁸ The spectrum of N 1s also illustrates the smaller contribution of positively charged N (-N^+) and the relatively larger contribution of neutral N (-N), and the ratio of $\text{-N}^+/\text{-N}$ was 0.49 for AGJ. However, after the adsorption of Cr(VI), the ratio of $\text{-N}^+/\text{-N}$ decreased to 0.37 (see Fig. 7d). This result indicates that the uptake of Cr(VI) by AGJ can be attributed to electrostatic attraction through the tertiary amine group.

The overall findings suggest that the adsorption of Cr(VI) on AGJ was not a simple, single process. The predominant mechanism might be chemisorption *via* amine, hydroxyl and/or the additional chemical functional groups of AGJ. Moreover, some other kinds of interactions, such as ion exchange, chemical bonding, hydrogen bonding and physical adsorption, also might be involved.

CONCLUSION

In this work, the adsorption performance of low-cost amino grafted jute stalks was investigated for the removal of Cr(VI) from aqueous solution. The results showed that the adsorption of Cr(VI) onto AGJ increased with increasing adsorbent dosage, but decreased with increasing initial solution pH. The kinetic data were perfectly described by the pseudo-second-order model, indicating the occurrence of a chemical adsorption process. The equilibrium adsorption data at different temperatures fitted best to the Langmuir isotherms. The maximum adsorption capacity of AGJ for Cr(VI) was found to be 154.30 mg/g. The nature of possible interactions between the adsorbent and the metal ion was examined by FTIR spectroscopy. It revealed the involvement of

-OH, -NH_2 and -COOH groups in chromium binding onto the AGJ surface. Also, the results from XPS analysis revealed that a part of the adsorbed Cr(VI) onto the AGJ surface was reduced to less toxic Cr(III), and the reduced Cr(III) was then adsorbed onto the surface of AGJ. Besides that, as the adsorbent was developed from a low-cost lignocellulose-rich agricultural waste, it could be burned after Cr(VI) adsorption, without further regeneration, which would help reduce the cost of waste disposal. Therefore, it can be concluded that AGJ could serve as a potential adsorbent for chromium removal from aqueous solutions.

ACKNOWLEDGMENTS: The authors are grateful for the financial support from National Natural Science Foundation of China (31601351), the Hunan Natural Science Foundation (2017JJ3349 and 2017JJ3350), the Science and Technology Innovation Project of Chinese Academy of Agricultural Sciences (CAAS-ASTIP-2017-IBFC01 and CAAS-XTCX2016016-2), National Hemp Industry Technical System (CARS-16-E01), the Germplasm Resources Protection Project (2016NWB044) and Central Public-Interest Scientific Institution Basal Research Fund (1610242019003).

REFERENCES

- 1 G. Bayramoglu and M. Y. Arica, *Chem. Eng. J.*, **139**, 20 (2008), <https://doi.org/10.1016/j.cej.2007.07.068>
- 2 S. H. Chen, Q. Y. Yue, B. Y. Gao, Q. Li, X. Xu *et al.*, *Bioresour. Technol.*, **113**, 114 (2012), <https://doi.org/10.1016/j.biortech.2011.11.110>
- 3 W. F. Liu, J. Zhang, C. L. Zhang and L. Ren, *Chem. Eng. J.*, **189**, 295 (2012), <https://doi.org/10.1016/j.cej.2012.02.082>
- 4 Y. A. Aydin and N. D. Aksoy, *Chem. Eng. J.*, **151**, 188 (2009), <https://doi.org/10.1016/j.cej.2009.02.010>
- 5 V. K. Gupta, A. Rastogi and A. Nayak, *J. Colloid. Interf. Sci.*, **342**, 135 (2010), <https://doi.org/10.1016/j.jcis.2009.09.065>
- 6 J. Yoon, G. Amy, J. Chung, J. Sohn and Y. Yoon, *Chemosphere*, **77**, 228 (2009), <https://doi.org/10.1016/j.chemosphere.2009.07.028>
- 7 H. Ozaki, K. Sharma and W. Saktaywin, *Desalination*, **144**, 287 (2002), [https://doi.org/10.1016/S0011-9164\(02\)00329-6](https://doi.org/10.1016/S0011-9164(02)00329-6)
- 8 B. Mukhopadhyay, J. Sundquist and R. J. Schmitz, *J. Environ. Manage.*, **82**, 66 (2007), <https://doi.org/10.1016/j.jenvman.2005.12.005>
- 9 E. Pehlivan and S. Cetin, *J. Hazard. Mater.*, **163**,

- 448 (2009), <https://doi.org/10.1016/j.jhazmat.2008.06.115>
- ¹⁰ Y. M. Qu, X. M. Zhang, J. Xu, W. J. Zhang and Y. Guo, *Sep. Purif. Technol.*, **136**, 10 (2014), <https://doi.org/10.1016/j.seppur.2014.07.054>
- ¹¹ X. J. Hu, J. S. Wang, Y. G. Liu, X. Li, G. M. Zeng *et al.*, *J. Hazard. Mater.*, **185**, 306 (2011), <https://doi.org/10.1016/j.jhazmat.2010.09.034>
- ¹² M. Bansal, D. Singh and V. K. Garg, *J. Hazard. Mater.*, **171**, 83 (2009), <https://doi.org/10.1016/j.jhazmat.2009.05.124>
- ¹³ L. C. Zheng, C. F. Zhu, Z. Dang, H. Zhang, X. Y. Yi *et al.*, *Carbohydr. Polym.*, **90**, 1008 (2012), <https://doi.org/10.1016/j.carbpol.2012.06.035>
- ¹⁴ M. Gorgievski, D. Bozic, V. Stankovic, N. Strbac and S. Serbula, *Ecol. Eng.*, **58**, 113 (2013), <https://doi.org/10.1016/j.ecoleng.2013.06.025>
- ¹⁵ Y. N. Chen, L. C. Ding and J. X. Nie, *Desalin. Water Treat.*, **44**, 168 (2012), <https://doi.org/10.1080/19443994.2012.691694>
- ¹⁶ I. Anastopoulos, A. Bhatnagar, B. H. Hameed, Y. S. Ok and M. Omirou, *J. Mol. Liq.*, **240**, 179 (2017), <https://doi.org/10.1016/j.molliq.2017.05.063>
- ¹⁷ I. Anastopoulos, M. Karamesouti, A. C. Mitropoulos and G. Z. Kyzas, *J. Mol. Liq.*, **229**, 555 (2017), <https://doi.org/10.1016/j.molliq.2016.12.096>
- ¹⁸ P. S. Vassileva, A. K. Detcheva, T. H. R. Radoykova, I. A. Avramova, K. I. Aleksieva *et al.*, *Cellulose Chem. Technol.*, **52**, 633 (2018), [http://www.cellulosechemtechnol.ro/pdf/CCT7-8\(2018\)/p.633-643.pdf](http://www.cellulosechemtechnol.ro/pdf/CCT7-8(2018)/p.633-643.pdf)
- ¹⁹ M. Sarkar, A. K. M. L. Rahman and N. C. Bhoumik, *Water Resour. Ind.*, **17**, 1 (2017), <https://doi.org/10.1016/j.wri.2016.12.003>
- ²⁰ A. Roy, B. Adhikari and S. B. Majumder, *Ind. Eng. Chem. Res.*, **52**, 6502 (2013), <https://doi.org/10.1021/ie400236s>
- ²¹ S. R. Shukla and R. S. Pai, *Bioresour. Technol.*, **96**, 1430 (2005), <https://doi.org/10.1016/j.biortech.2004.12.010>
- ²² Y. Hao, Z. P. Cui, H. Yang, G. B. Guo, J. Y. Liu *et al.*, *Cellulose Chem. Technol.*, **52**, 485 (2018), [http://www.cellulosechemtechnol.ro/pdf/CCT5-6\(2018\)/p.485-494.pdf](http://www.cellulosechemtechnol.ro/pdf/CCT5-6(2018)/p.485-494.pdf)
- ²³ Z. L. Du, T. Zheng, P. Wang, L. L. Hao and Y. X. Wang, *Bioresour. Technol.*, **201**, 41 (2016), <https://doi.org/10.1016/j.biortech.2015.11.009>
- ²⁴ M. Zheng, Y. Ahn, Y. Yoon, W. K. Park, Y. Jung *et al.*, *Sep. Sci. Technol.*, **51**, 2958 (2016), <https://doi.org/10.1080/01496395.2016.1231693>
- ²⁵ S. H. Chen, Q. Y. Yue, B. Y. Gao, Q. Li and X. Xu, *Chem. Eng. J.*, **168**, 909 (2011), <https://doi.org/10.1016/j.cej.2011.01.063>
- ²⁶ X. Y. Guo, S. Z. Zhang and X. Q. Shan, *J. Hazard. Mater.*, **151**, 134 (2008), <https://doi.org/10.1016/j.jhazmat.2007.05.065>
- ²⁷ K. K. Singh, M. Talat and S. H. Hasan, *Bioresour. Technol.*, **97**, 2124 (2006), <https://doi.org/10.1016/j.biortech.2005.09.016>
- ²⁸ Z. F. Ren, X. Xu, X. Wang, B. Y. Gao, Q. Y. Yue *et al.*, *J. Colloid. Interf. Sci.*, **468**, 313 (2016), <https://doi.org/10.1016/j.jcis.2016.01.079>
- ²⁹ L. L. Hao, T. Zheng, J. P. Jiang, Q. Hu, X. L. Li *et al.*, *RSC Adv.*, **5**, 10723 (2015), <https://doi.org/10.1039/c4ra11901k>
- ³⁰ L. V. A. Gurgel, J. C. P. de Melo, J. C. de Lena and L. F. Gil, *Bioresour. Technol.*, **100**, 3214 (2009), <https://doi.org/10.1016/j.biortech.2009.01.068>
- ³¹ A. M. Yusof and N. A. N. N. Malek, *J. Hazard. Mater.*, **162**, 1019 (2009), <https://doi.org/10.1016/j.jhazmat.2008.05.134>
- ³² Q. Q. Zhong, Q. Y. Yue, B. Y. Gao, Q. Li and X. Xu, *Chem. Eng. J.*, **229**, 90 (2013), <https://doi.org/10.1016/j.cej.2013.05.083>
- ³³ S. H. Chen, Q. Y. Yue, B. Y. Gao and X. Xu, *J. Colloid. Interf. Sci.*, **349**, 256 (2010), <https://doi.org/10.1016/j.jcis.2010.05.057>
- ³⁴ M. W. Wan, C. C. Kan, B. D. Rogel and M. L. P. Dalida, *Carbohydr. Polym.*, **80**, 891 (2010), <https://doi.org/10.1016/j.carbpol.2009.12.048>
- ³⁵ M. Y. Chang and R. S. Juang, *Colloid. Surface. A*, **269**, 35 (2005), <https://doi.org/10.1016/j.colsurfa.2005.06.064>
- ³⁶ N. Tolazzi, E. Steffani, E. Barbosa-Coutinho, J. B. S. Junior, J. C. Pinto *et al.*, *Chem. Eng. Res. Des.*, **138**, 144 (2018), <https://doi.org/10.1016/j.cherd.2018.08.027>
- ³⁷ G. O. Cassol, R. Gallon, M. Schwaab, E. Barbosa-Coutinho, J. B. Severo *et al.*, *Adsorpt. Sci. Technol.*, **32**, 257 (2014), <https://doi.org/10.1260/0263-6174.32.4.257>
- ³⁸ C. Y. Kuo, C. H. Wu and J. Y. Wu, *J. Colloid. Interf. Sci.*, **327**, 308 (2008), <https://doi.org/10.1016/j.jcis.2008.08.038>
- ³⁹ C. H. Deng, J. L. Gong, G. M. Zeng, Y. Jiang, C. Zhang *et al.*, *Chem. Eng. J.*, **284**, 41 (2016), <https://doi.org/10.1016/j.cej.2015.08.106>
- ⁴⁰ N. Daneshvar, D. Salari and S. Aber, *J. Hazard. Mater.*, **94**, 49 (2002), [https://doi.org/10.1016/S0304-3894\(02\)00054-7](https://doi.org/10.1016/S0304-3894(02)00054-7)
- ⁴¹ N. Shevchenko, V. Zaitsev and A. Walcarius, *Environ. Sci. Technol.*, **42**, 6922 (2008), <https://doi.org/10.1021/es800677b>